Polarization Switching and Negative Capacitance in Epitaxial $PbZr_{0.2}Ti_{0.8}O_3$ Thin Films

Lucian Pintilie, Georgia Andra Boni,* Cristina Chirila, Luminita Hrib, Lucian Trupina, Lucian Dragos Filip, and Ioana Pintilie
National Institute of Materials Physics, Atomistilor 405A, Magurele 077125, Romania

(Received 5 April 2020; revised 3 June 2020; accepted 5 June 2020; published 27 July 2020)

The negative-capacitance effect in devices based on combined ferroelectric-dielectric gate oxides is thought to be a potential solution to break free from the so-called Boltzmann tyranny. To lower the power consumption in field-effect transistors, the subthreshold swing factor S should be reduced below the thermodynamic limit of 60 mV per decade. Yet, despite numerous studies dedicated to this effect in the past decade, its origin in ferroelectric capacitors or ferroelectric-based superlattices remains unclear, being considered either a transitory product of polarization switching or an intrinsic phenomenon related to the presence of ferroelectric polarization. In this study it is shown, starting from simple electrostatic considerations, that negative capacitance is present during polarization switching and is accompanied by a significant increase of the current flowing through the ferroelectric capacitor. Coupled with piezo-force microscopy results, it is shown that the polarization orientation suddenly changes at the coercive voltage, accompanied by a complete reconfiguration of the potential barriers at the Schottky-like contacts present at the electrode-ferroelectric interfaces. A method to estimate the polarization-switching time, as the time associated with the presence of the negative-capacitance effect, is proposed. Values in the range from 100 to 1000 ns are obtained for epitaxial $PbZr_{0.2}Ti_{0.8}O_3$ films. These findings suggest that negative capacitance may be an intrinsic effect in ferroelectrics but that it is a transitory effect, present only when ferroelectric polarization passes through zero (switching).

DOI: 10.1103/PhysRevApplied.14.014080

I. INTRODUCTION

The phenomenon of negative capacitance (NC) was discovered in the 1960s in amorphous semiconductor chalcogenide thin films [1]. Since then, it has been reported in various systems, including Schottky diodes, solar cells, and metal-insulator-metal (*M-I-M*) structures [2–8]. Its origin is still unclear, although several explanations have been suggested, such as the following: inductive behavior at low frequencies in impedance spectroscopy, leading to opposite variations of voltage and charge [3,9]; the current time response to a steplike bias, which can lead to NC if the transient current increases while the voltage is decreased [10]; the variation of the charge trapped on interface states due to impact ionization [2]; and nonequilibrium carrier injection in the case of quantum wells, leading to current transients [11]. Regarded at the beginning as an exotic phenomenon, the interest in negative capacitance has exploded since it has been suggested that it may exist in ferroelectrics and may be useful to overcome the thermodynamic limit of 60 mV per decade in the slope of the subthreshold (S) characteristic of a field-effect transistor (FET) [12]. In other words, if a ferroelectric is combined with a dielectric as gate layers in a FET structures, then a voltage amplification may occur in the ferroelectric, leading to significantly lower slopes and thus leading to significant reduction of the energy budget in the FET. Since then, hundreds of papers have been published, claiming S values as low as about 10 mV per decade [13,14].

However, to this day, there are two fundamental questions that are yet to be answered definitively:

(i) Is "negative capacitance" a true physical effect or just an artifact due to some sudden changes in the charge transport through the tested structure?

(ii) Is "negative capacitance" a transitory effect or can it be stabilized in the steady state?

Before going further, one has to remember that, in the specific case of ferroelectrics, the presence of NC is related to the double-well shape of the free-energy dependence on the order parameter (dielectric displacement or ferroelectric polarization). Thermodynamic theory predicts that the double derivative of the free energy, meaning the permittivity, should be negative at polarization values around zero, where the free energy has a maximum [15,16].

*andra.boni@infim.ro

Many structures and experiments have been designed to respond to the two questions mentioned above. For example, steady-state NC has been reported in ferroelectric-dielectric superlattices [17,18]. In other experiments, transient NC has been demonstrated in the case of ferroelectric capacitors in series with passive resistors or capacitors [19–22]. NC has also been claimed in dielectric-ferroelectric multilayers, based on the fact that the capacitance of the structure is larger than that expected from the simple serial model of capacitors or than that expected from a capacitor having the same dielectric and the same thickness as the multilayer [23,24]. In all these cases, the presence of NC has been attributed to the ferroelectric component being placed in situations where the polarization value is near zero, as happens near the phase transition or near the coercive voltage or field.

However, there are also studies that question the presence of the NC effect, and suggest that it may be an artifact associated with resistive and/or capacitive elements coupled to the ferroelectric layer or that it may be related to the presence of interface charges that can lead to a higher capacitance in superlattices than that estimated from the serial model of capacitances [25–27]. Nevertheless, it is clear that, despite numerous efforts dedicated to the understanding of the physical nature of the NC effect in ferroelectric structures, this phenomenon still remains elusive and far from any real-life applications.

II. MATERIALS AND METHODS

The samples used for the present study are epitaxial $PbZr_{0.2}Ti_{0.8}O_3$ (PZT) thin films with a thickness of 50 nm, grown by pulsed-laser deposition (PLD) on a single-crystal $SrTiO_3$ (STO) substrate with an (001) orientation, and having a bottom $SrRuO_3$ (SRO) electrode layer with a thickness of 20 nm, deposited by the same method. The capacitor structure is completed by the deposition of a top SRO contact with an area of $100 \times 100\ \mu m^2$. Details of the deposition parameters and the structural quality of the deposited films can be found in previously published papers [28,29].

The capacitance-voltage (*C-V*) characteristics are measured using a Hioki 3536 LCR bridge connected to a Keithley 6517 electrometer with an incorporated *dc* voltage source for the incremental application of a *dc* voltage to the sample. The measurements are performed using an *ac* signal with a frequency of 100 kHz and with an amplitude of 0.05 V. The ferroelectric characterization is performed using a TF2000 Ferritester Analyzer, in positive up negative down and/or pulse mode. The electrical measurements are performed by placing the sample inside a cryogenic probe station (from Lake Shore) with micromanipulated arms and by contacting the bottom and top electrodes with Cu-Be needles. All the measurements are performed at room temperature and in a normal atmosphere.

For the piezoresponse-force microscopy (PFM) studies, an MFP-3D-SA microscope (from Asylum Research) is used in dual ac resonance tracking (DART) mode. An OMCL-AC 240TM cantilever is used, with a spring constant of $2\ N\,m^{-1}$ and a resonant frequency of 70 kHz.

III. RESULTS

Here, we present our contributions to this very hot topic by analyzing in detail the polarization hysteresis loops and the processes taking place during switching and discussing possible alternatives for what it is actually interpreted as NC in ferroelectric capacitors or related structures. The starting point is the relation between the dielectric displacement D, the electric field E, and the dielectric polarization P [30,31]:

$$D = \varepsilon_0 E + P, \tag{1}$$

where ε_0 is the vacuum permittivity, and P is the total polarization, including the linear part P_L specific for any dielectric and/or semiconductor material and the nonlinear ferroelectric part characterized by the spontaneous polarization P_S. Replacing P_L with $\varepsilon_0 \chi E$ (where χ is the electric susceptibility), Eq. (1) can be written as

$$D = \varepsilon_0(1+\chi)E + P_S = \varepsilon_0 \varepsilon_b E + P_S. \tag{2}$$

Here, ε_b is the background static dielectric constant of the ferroelectric. The total static dielectric constant of a ferroelectric ε_f can be defined as

$$\varepsilon_f = \varepsilon_b + \frac{1}{\varepsilon_0}\frac{\partial P_S}{\partial E}. \tag{3}$$

In this form, Eq. (3) provides some important clues:

(i) if the spontaneous polarization is saturated (i.e., no longer changes with the applied electric field), $\varepsilon_f = \varepsilon_b$.

(ii) ε_f can be negative if the derivative of the spontaneous polarization with respect to the applied electric field is negative (e.g., the polarization increases when the electric field decreases).

(iii) The electric field dependence of the dielectric constant is the derivative of the ferroelectric hysteresis loop (in other words, the *C-V* characteristics should be the derivative of the *D-E* or *P-E* loop, assuming that the term $\varepsilon_0 E$ in Eq. (1) is negligible).

Typical hysteresis loops for the polarization and the current are presented in Fig. 1(a). The polarization value is high and similar to the values reported in the literature. A significant internal electric field is present in the film, as suggested by the shift of the hysteresis loops toward positive voltage values. Considering that the top SRO electrode

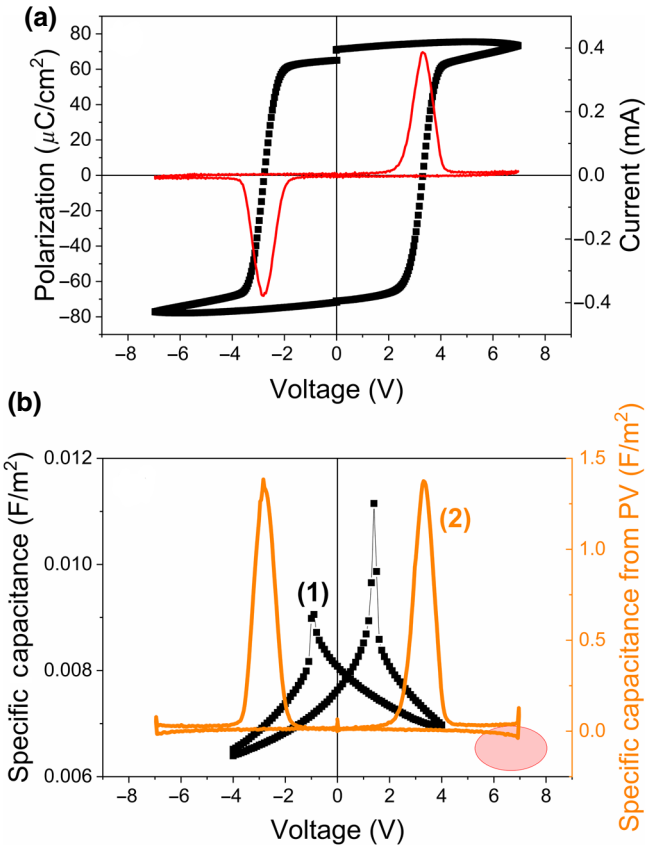

FIG. 1. (a) Polarization and current hysteresis loops obtained for a SRO/PZT/SRO ferroelectric capacitor by applying a triangular voltage pulse with a frequency of 1 kHz. (b) The *C-V* characteristics obtained by direct measurement of capacitance using an ac signal of 0.1 V amplitude and 10 kHz frequency, while the dc voltage is modified step by step [marked (1)], and the *C-V* characteristic obtained by deriving the polarization hysteresis presented in Fig. 1(a) [marked as (2)].

is the "hot" contact, one can deduce that the internal electric field is oriented from the bottom SRO contact toward the top one. Figure 1(b) presents the*C-V* characteristic obtained on the same contact, together with the *C-V* "characteristic" obtained by deriving the polarization hysteresis loop shown in Fig. 1(a).

Figure 1(b) reveals some interesting aspects:

(a) The shape of the directly measured *C-V* characteristic is totally different compared to the shape of the characteristic obtained by deriving the polarization hysteresis loop; the capacitance peaks associated with polarization switching are very sharp in the case of the directly measured *C-V* characteristic, with a sudden change in the capacitance value after switching.

(b) The capacitance values normalized to the electrode area are very different; there is a 2-order-of-magnitude difference between the ones obtained from the derived *C-V* characteristic and the ones that are directly measured.

(c) In the case of the directly measured *C-V* characteristic, the capacitance still varies with the applied voltage after polarization switching, while in the case of the derived characteristic the capacitance value seems to remain constant with voltage, except for the interval where the switching takes place.

(d) NC values are present in the case of the derived *C-V* characteristic [marked with a circle in Fig. 1(b)].

The last observation leads to more detailed experiments such as the one in Fig. 2(a), showing intermediate hysteresis loops. A careful analysis of the circled areas in Fig. 2(a) reveals that the polarization still increases while the applied voltage decreases from the maximum applied value toward zero. This is the fingerprint of NC!. Indeed, the derivatives of the hysteresis loops presented in Fig. 2(a) exhibit clear negative values in the voltage range where polarization switching takes place(roughly between 1.5 V and 3.8 V, with the coercive voltage around 3 V), as shown in Fig. 2(b). One can also see that NC has a maximum value at voltages roughly equal to the coercive value. This is in agreement with the findings that NC is more visible if the value of P is close to zero [18].

Moving further, an even more interesting evolution is that of the current hysteresis shown in Fig. 3(a), especially near the maximum applied voltage [see the inset in Fig. 3(a)], where the arrow evidences the increase and decrease of the current recorded during the hysteresis measurements, at voltages near the maximum applied one. Figure 3(b) explicitly shows that there is a direct correlation between NC and the current recorded during the hysteresis measurement: when NC reaches its maximum value, the current is also a maximum.

Another interesting result is obtained if the voltage dependence is converted into a time dependence, given the knowledge that all the hysteresis measurements are performed with triangular voltage pulses at 1 kHz and thus the voltage varies linearly in time between zero and maximum amplitudes for positive and negative polarities [see also the inset in Fig. 2(a)]. Then, for each quarter $V = \alpha t$, where the voltage variation rate α can be obtained with knowledge of the amplitude of the applied triangular voltage pulse V_{max} and its frequency, resulting in $\alpha = 4fV_{max}$. The real rate for the voltage change will change the sign when the voltage is increasing from 0 to V_{max} and is decreasing from V_{max} to 0, but in absolute-value terms, it remains the same. Therefore, the time t that elapses from the moment $t = 0$ when the measurement starts until the applied voltage reaches a value V is obtained as $t = V/4fV_{max}$. Applying this procedure to the points marked with arrows in Fig. 3(b), the times $t1$ and $t2$ can be calculated. The difference $t2 - t1$ can be regarded as the polarization-switching time, considering that NC exists as a nonzero quantity only during switching. The obtained values for several contacts on the same sample are in the range from 200 to 500 ns,

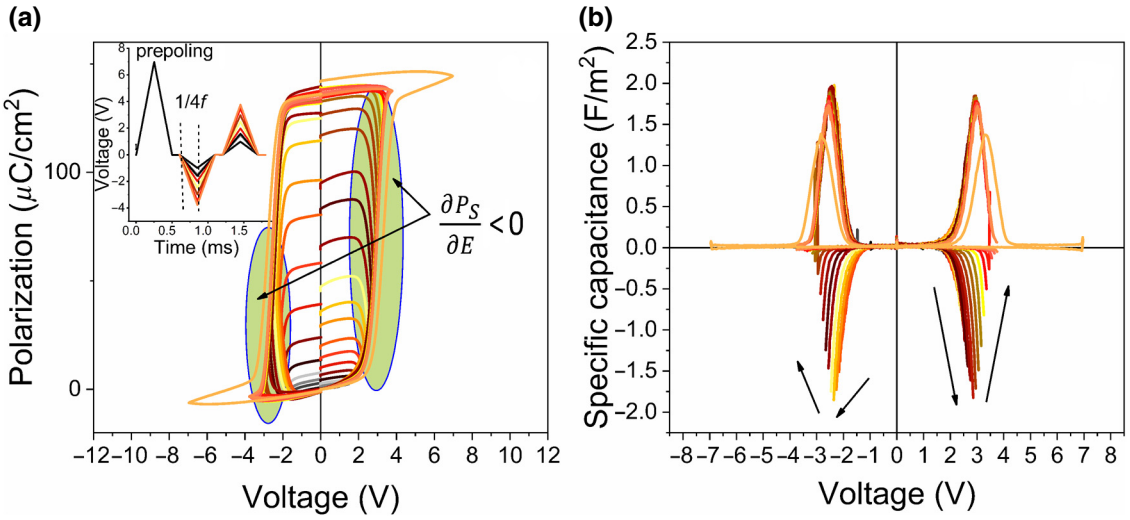

FIG. 2. (a) The opening of the polarization hysteresis loop as the amplitude of the triangular voltage pulse is gradually increased (the red arrow marks the increase). (b) The *C-V* characteristics derived from the hysteresis loops presented in (a). The arrows mark the increase and decrease of NC observed for voltages corresponding to the domains marked in (a).

showing that switching is very fast and probably dependent on the structural quality of the film beneath the measured contact (since structural defects may act as pinning centers, making the switching more difficult, which is reflected in longer switching times).

So far, all the conclusions are drawn from classical electrical measurements; however, equally interesting results are obtained if specially designed PFM measurements are used to observed the switching process at the microscopic level. The results are summarized in Fig. 4, revealing that during switching, there is no mix of ferroelectric domains of different orientations, the polarization going very rapidly from one orientation to the other. The map of the poling voltage is shown in Fig. 4(a) and the voltage variation during the scan along the line in Fig. 4(a) is shown in Fig. 4(b). Figure 4(c) shows the phase contrast after applying the poling map from Fig. 4(a). The image is a little shifted due to the low scan rate, which is only 0.5 Hz. In any case, one can see an outer white frame associated with the poling voltage of +5.33 V and an inner black frame associated with the poling voltage of −5.33 V. Inside the frames, two dominant regions can

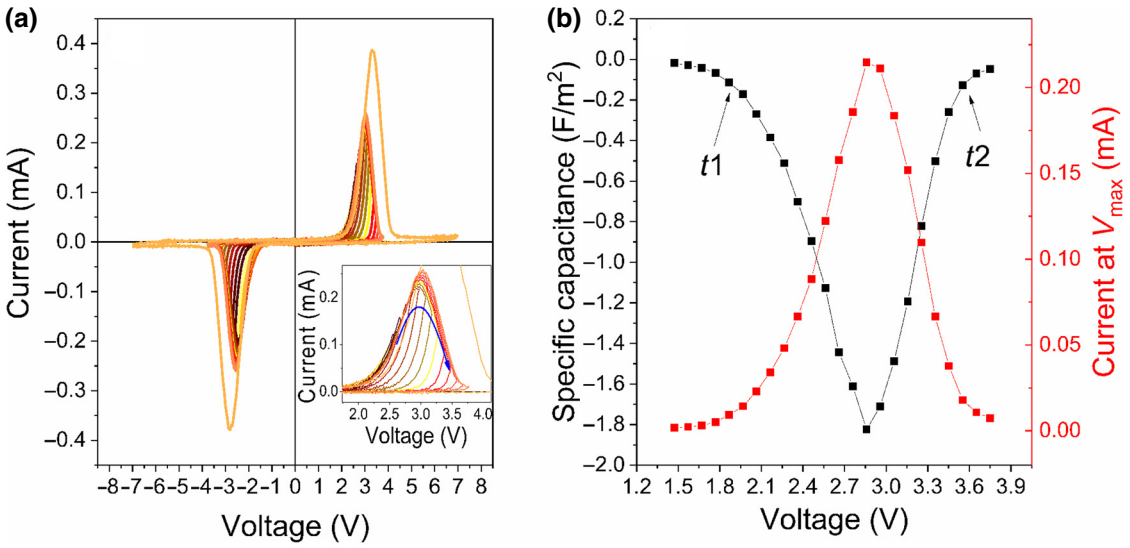

FIG. 3. (a) The current hysteresis recorded at the same time as the polarization-hysteresis measurements in Fig. 2(a). (b) The voltage dependence of the maximum value of NC in the positive voltage range [see also the arrows in Fig. 2(a)], together with the voltage dependence of the current recorded at the maximum applied voltage during the hysteresis measurement.

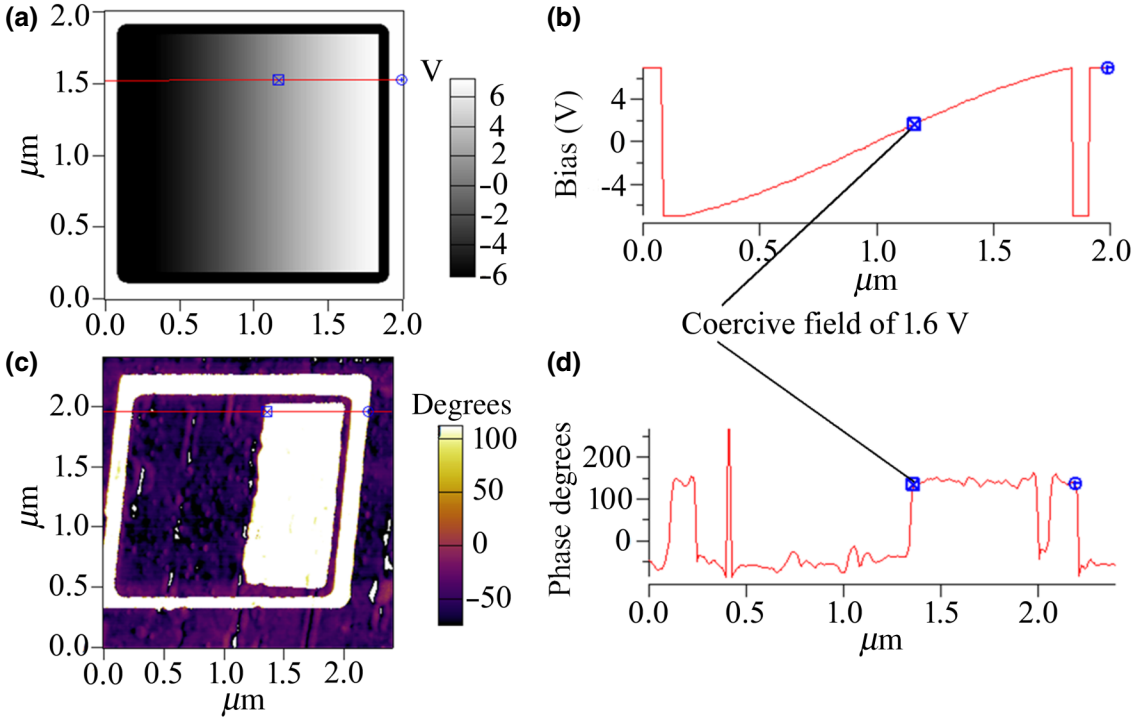

FIG. 4. (a) The poling map. (b) The voltage variation while the PFM tip scans the line in (a)—it starts at +5.33 V, then after about 0.1 μm drops to −5.33 V and starts to slowly increase to +5.33 V while the tip is moving on the surface of the sample, after which it drops again to −5.33 V for about 0.1 μm and suddenly changes to +5.33 V for the final 0.1 μm. (c) The phase contrast after applying the poling map from (a). (d) The phase variation while the tip scans the line in (c).

distinguished: one black, corresponding to voltages from −5.33 V to +1.6 V; and one white, for voltages from +1.6 V up to +5.33 V. Inside the two regions are points or lines of opposite color, suggesting different polarization orientations compared to the rest of the region [see also Fig. 4(d)], showing the phase variation during the scan along the line from Fig. 4(c).

These results suggest that the switching is abrupt, with no intermediate states composed of ferroelectric domains of different orientations. The findings presented above are, apparently, in contrast to existing theories claiming that the polarization switching between two states with completely opposite orientations takes place through a series of intermediate states composed of ferroelectric domains with opposite polarization orientations. However, one has to consider the time scale and the spatial resolution of the PFM characterization. For very fast switching, implying very fast nucleation and growth of domains, it may be that intermediate-domain structures are not visible during the time frame of the measurement (the time for a scan is 2 s; during this time, the voltage varies from −5.33 V to +5.33 V). In discussing and explaining the experimental results, one has to take into account that the analyzed structure is metal-ferroelectric-metal (*M-F-M*) and that the electrode-ferroelectric interfaces behave as Schottky-like contacts. The ferroelectric polarization affects the band bending at the interfaces in the sense that for the interface where polarization ends with a positive surface charge, the band bending is lower than for the interface where the polarization ends with a negative surface charge. These assumptions are valid for an *n*-type semiconductor and epitaxial PZT is thought to be of *n* type due to oxygen vacancies formed by self-doping to preserve the out-of-plane orientation of the polarization [28] (it is documented in the literature that epitaxial PZT grown on STO/SRO substrates has out-of-plane polarization oriented from the substrate toward the surface). Therefore, the band bending at a ferroelectric Schottky-like contact is given by

$$V'_{\mathrm{bi}} = V_{\mathrm{bi}} - \frac{P}{\varepsilon_0 \varepsilon_{\mathrm{st}}}\delta, \tag{4}$$

where V'_{bi} is an apparent built-in potential, V_{bi} is the built-in potential in the absence of polarization, P is the polarization, ε_0 is the vacuum permittivity, $\varepsilon_{\mathrm{st}}$ is the low-frequency dielectric constant, and δ is the thickness of the interface layer (the layer between the polarization bound charges and the physical electrode interface). When the polarization charges are positive, they will attract more electrons for compensation and the band bending will be reduced, as well as the thickness of the depleted region. If the polarization charges are negative, then electrons will be repelled from the interface and the band bending will increase, as well as the thickness of the depleted region.

If the polarization is zero, then the built-in potential is not altered.

The question is: How can Schottky-like contacts explain the occurrence of NC during polarization switching and the fact that this process takes place directly from $+P$ to $-P$ or vice versa, without apparent intermediate states characterized by a mix of domains with opposite orientations? To answer this question, one has to consider the present interpretation of polarization switching based on the nucleation-and-growth model. There are three main steps during switching from one monodomain state to the other monodomain state:

(1) The nucleation of domains of opposite polarization orientation. This is thought to happen on structural defects from the bulk and interfaces. If the bulk is free of defects, then nucleation takes place at electrode interfaces.

(2) The growth of the domains of opposite polarization orientation until the new monodomain state is attained.

(3) The compensation of the depolarization field established during switching and just after the switching is completed. This is achieved with carriers existing inside the ferroelectric film or in the external circuit (electrodes), carriers that can move from one electrode interface to the other.

The results presented in this study suggest that the first step, nucleation, takes place at the electrode interface over the entire area of the electrode, followed by the second step, growth. In practice, the polarization switches very rapidly from one direction to the other, with the zero-polarization state assumed to happen when the polarization in half of the volume has switched while that in the other half has not. The lifetime of the zero-polarization state is very short, since this state is not thermodynamically stable, according to the theoretical models [17]. This means that the external electric field applied on the *M-F-M* structure pushes the system from the energy minima corresponding to $+P$ to the minima corresponding to $-P$ and vice versa, with no intermediate values for P.

The first two steps of polarization switching, nucleation and growth, are supposed to be very fast (hundreds of picoseconds) [32]. The third step, compensation of the depolarization field, appears to be the longer one, since it involves charge redistribution from one electrode interface to the other.

The relation between NC and the increase of the current during switching [see Fig. 3(b)] can be explained on the basis of Eq. (4). We only discuss what happens at one electrode interface, since the same process is valid for the other interface—it is only the sign of the charges that changes. Let us then assume that the polarization is in the up direction, meaning a positive polarization charge at the top interface. The built-in potential will be reduced, according to Eq. (4). The switching involves a sudden (or very rapid) change from a positive to a negative polarization charge, with a corresponding change in the magnitude of the built-in potential and depletion width. It also involves a replacement of the negative charges that are initially present at the top interface to compensate the positive polarization charges with positive charges. This triggers a rapid increase of the current flowing through the circuit, which reaches a maximum when it appears that the system is passing through the state with zero polarization. At this point, $V'_{bi} = V_{bi}$, according to Eq. (4); then opposite polarization (down) occurs, leading to a sharp increase of the apparent built-in potential and to a drop of the current magnitude. However, the current variation is continuous during switching due to the fact that charges are continuously flowing through the circuit to compensate the depolarization field during switching. The sharp changes in the apparent built-in potential are visible in the *C-V* characteristics presented in Fig. 1(b) ["(1)" on the graph]. One can note that the capacitance value decreases sharply after switching, which is correlated with the increase of the apparent built-in potential and the increase of the depletion width.

In order to better understand the discussion related to Eq. (4), the successive steps taking place inside the structure during polarization switching are represented schematically in Fig. 5. Starting from the top, the charge density at the two interfaces is shown with changing color gradients, to correlate with Eq. (4):

(a) The initial state, with a well-defined orientation of polarization, from left to right in the present case, and with well-defined space charge regions at the electrodes.

(b) The polarization state at electric fields below the coercive values, but of opposite orientation compared to the polarization; the direction of polarization is still maintained but the width of the depletion regions starts to change as the applied voltage increases.

(c) The polarization state at electric fields around the coercive value; the polarization is near zero, with significantly reduced depletion regions at the electrode interfaces, allowing a significant flow of charge (high current), as suggested by the small blue arrows at the electrodes.

(d) Polarization switching to the opposite direction, with an applied electric field higher than the coercive value; the depletion barriers are restored, leading to a significantly reduced flow of charge (low current).

Using the visual representation in Fig. 5, polarization switching takes place in three successive steps starting from the moment an external electric field E is applied to the system in Fig. 5(b):

(a) Free electrons will start to accumulate at the left interface, reducing the depletion region, while at the right interface electrons will be injected, adding to the already

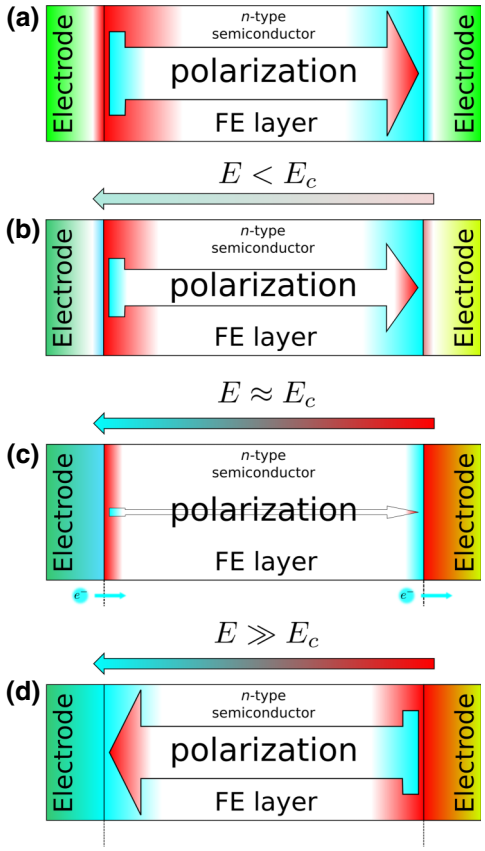

FIG. 5. A sketch of an electrode/PZT/electrode capacitor, showing the polarization charges (light blue, negative charges; red, positive charges), external electric fields, depleted regions (red gradient), and "clouds" of free charges compensating the bound polarization charges (light blue gradient) in four situations: (a) the initial state of the PZT film; (b) the start of the polarization switching by the application of a reverse electric field; and (c) a ferroelectric near the switching point. The incoming (left interface) and outgoing (right interface) charge transfer destabilizes the charge compensation of polarization until polarization switching takes place in (d). At this point, at the right interface, the depletion region is formed to compensate the negative polarization charges while at the left interface an electron accumulation appears to complete the polarization compensation.

existing electrons that compensate the $+P$ polarization charges. As the external electric field is increased, more electrons will be injected through the right interface and extracted to the left interface, leading to an increase of the current.

(b) When the external electric field reaches the coercive value, polarization is now zero (ideally) and there will be no polarization influence on the built-in potential and on the width of the depletion regions; thus the current will have reached its peak, while negative capacitance is also at a maximum. This is an unstable thermodynamic state, where the structure behaves more like a resistor than a capacitor. In the free-energy landscape, it is the state corresponding to the concave local maximum $P = 0$, from which the system can equally go into one of the stable energy minima, each corresponding to one polarization orientation. Further increase of the external electric field pushes the system into the minimum corresponding to the opposite polarization direction compared to the initial one.

(c) The polarization rapidly saturates after switching, being accompanied by the reappearance of the depletion region at the right interface and of the electron cloud at the left interface. Once the polarization-controlled depletion regions are re-established and the necessary compensation charges redistributed, the current flow decreases and the NC effect vanishes.

IV. CONCLUSIONS

Several conclusions can be drawn based on the above results and analysis:

(1) Experimentally measured P-V and C-V loops do not verify the theoretical prediction that $C(V)$ dependence is obtained as the derivative of the $P(V)$ dependence. While Eqs. (1)–(3) are deduced using electrostatic theory, the experimental methods used for P-V and C-V measurements are dynamic and assume the application of a periodic time-varying voltage. The frequencies, amplitudes, and shapes of the periodic voltage signals used for the two types of measurements are different; thus one cannot apply the theoretical deduction that the C-V characteristic is the derivative of the P-V loop for experimentally recorded results.

(2) Polarization switching is very fast in epitaxial films, the switching time being of the order of 100 ns.

(3) Switching starts from the interface where, most probably, the Schottky-like contact disappears and the compensation charge is no longer stable.

(4) The PFM results presented in Fig. 4 suggest that the switching takes place without visible intermediate states composed of up and down polarization; apparently, the system just switches from up to down polarization or vice versa. The $P = 0$ state, if present, is not stable and the system changes rapidly from one polarization orientation to the other.

(5) NC occurs only during switching. Its amplitude and temporal extension may depend on the structural quality of the electrode interfaces and of the films itself. In essence, NC is intrinsically related to polarization switching and occurs due to a large increase of the current due to the redistribution of the charges that compensate the depolarization field. The magnitude of NC may depend on the structural quality but it is always present as a transitory effect. It remains to be clarified if such an effect is useful in practical applications such as FETs for reduction of power consumption [12].

The present study supports the presence of an intrinsic transitory NC effect in epitaxial ferroelectric films, occurring around the coercive voltage when the polarization value is close to zero. However, the topic of the NC effect in relation to polarization switching is far from being closed. There are still many open questions, such as the following. What is the influence of structure quality (epitaxial, textured, or polycrystalline) on the NC effect? If one adopts the mechanism based on the occurrence of ferroelectric domains during switching, then the polarization values are the same in all the domains? (One can assume that different polarization values can be obtained from different volumes of domains with different orientations of polarization but with the same value of polarization.) Is it possible that the switching takes place without the formation of domains but just by moving the central atom (Ti or Zr) in the cell, from one off-center stable position to the other position along the *c* axis in the case of a tetragonal structure? (This can lead to different polarization values between maximum values associated with the two stable states of the central atom.) Switching through the formation of domains with the same polarization value seems to be supported by thermodynamic theory, in which only two minima exist in the free energy, all the other states being unstable. On the other hand, there are recent results suggesting the moving of the central atom as the mechanism for switching (including the present study) [33,34]. Further studies are needed to provide answers to the above questions, pushing the experiments to the limits of the existing equipment.

ACKNOWLEDGMENTS

We acknowledge the financial support of the Romanian Ministry of Research and Innovation through the PCCF Project No. PN-III-P4-ID-PCCF-2016-0047 funded by the Ministry of Research and Innovation through the Executive Agency for Higher Education, Research, Development and Innovation Funding (UEFISCDI) Executive Unit 6.

[1] R. Vogel and P. G. Walsh, Negative capacitance in amorphous semiconductor chalcogenide thin films, Appl. Phys. Lett. **14**, 216 (1969).

[2] X. Wu, E. S. Yang, and H. L. Evans, Negative capacitance at metal-semiconductor interfaces, J. Appl. Phys. **68**, 2845 (1990).

[3] H. C. F. Martens, J. N. Huiberts, and P. W. M. Blom, Simultaneous measurement of electron and hole mobilities in polymer light-emitting diodes, Appl. Phys. Lett. **77**, 1852 (2000).

[4] V. Kytin, T. Dittrich, F. Koch, and E. Lebedev, Injection currents and effect of negative capacitance in porous TiO_2, Appl. Phys. Lett. **79**, 108 (2001).

[5] B. K. Jones, J. Santana, and M. McPherson, Negative capacitance effects in semiconductor diodes, Solid State Commun. **107**, 47 (1998).

[6] J. Panigrahi, R. Singh Vandana, N. Batra, J. Gope, M. Sharma, P. Pathi, S. K. Srivastava, C. M. S. Rauthan, and P. K. Singh, Impedance spectroscopy of crystalline silicon solar cell: Observation of negative capacitance, Solar Energy **136**, 412 (2016).

[7] K. Shimizu, Y. Tanaka, Y. Noguchi, and H. Ishii, Negative capacitance in an organic solar cell observed by displacement current measurement, J. Phys.: Conf. Ser. **924**, 012012 (2017).

[8] F. Ebadi, N. Taghavinia, R. Mohammadpour, A. Hagfeldt, and W. Tress, Origin of apparent light-enhanced and negative capacitance in perovskite solar cells, Nat. Commun. **10**, 1 (2019).

[9] I. Mora-Seró, J. Bisquert, F. Fabregat-Santiago, G. Garcia-Belmonte, G. Zoppi, K. Durose, Y. Proskuryakov, I. Oja, A. Belaidi, T. Dittrich *et al.*, Implications of the negative capacitance observed at forward bias in nanocomposite and polycrystalline solar cells, Nano Lett. **6**, 640 (2006).

[10] A. K. Jonscher, The physical origin of negative capacitance, J. Chem. Soc. Faraday Trans. 2: Mol. Chem. Phys. **82**, 75 (1986).

[11] M. Ershov, H. Liu, L. Li, M. Buchanan, Z. Wasilewski, and A. Jonscher, Negative capacitance effect in semiconductor devices, IEEE Trans. Electron Devices **45**, 2196 (1998).

[12] S. Salahuddin and S. Datta, Use of negative capacitance to provide voltage amplification for low power nanoscale devices, Nano Lett. **8**, 405 (2008).

[13] F. A. McGuire, Z. Cheng, K. Price, and A. D. Franklin, Sub-60 mV decade^{-1} switching in 2D negative capacitance field-effect transistors with integrated ferroelectric polymer, Appl. Phys. Lett. **109**, 093101 (2016).

[14] L. Tu, X. Wang, J. Wang, X. Meng, and J. Chu, Ferroelectric negative capacitance field effect transistor, Adv. Electron. Mater. **4**, 1800231 (2018).

[15] C. M. Krowne, S. W. Kirchoefer, W. Chang, J. M. Pond, and L. M. B. Alldredge, Examination of the possibility of negative capacitance using ferroelectric materials in solid state electronic devices, Nano Lett. **11**, 988 (2011).

[16] S.-C. Chang, U. E. Avci, D. E. Nikonov, S. Manipatruni, and I. A. Young, Physical Origin of Transient Negative Capacitance in a Ferroelectric Capacitor, Phys. Rev. Appl. **9**, 014010 (2018).

[17] P. Zubko, J. C. Wojdeł, M. Hadjimichael, S. Fernandez-Pena, A. Sené, I. A. Luk'yanchuk, J.-M. Triscone, and J. Íñiguez, Negative capacitance in multidomain ferroelectric superlattices, Nature **534**, 524 (2016).

[18] A. K. Yadav, K. X. Nguyen, Z. Hong, P. García Fernández, P. Aguado-Puente, C. T. Nelson, S. Das, B. Prasad, D. Kwon, S. Cheema *et al.*, Spatially resolved steady-state negative capacitance, Nature **565**, 468 (2019).

[19] A. I. Khan, D. Bhowmik, P. Yu, S. J. Kim, X. Pan, R. Ramesh, and S. Salahuddin, Experimental evidence of ferroelectric negative capacitance in nanoscale heterostructures, Appl. Phys. Lett. **99**, 113501 (2011).

[20] A. I. Khan, K. Chatterjee, B. Wang, S. Drapcho, L. You, C. Serrao, S. R. Bakaul, R. Ramesh, and S. Salahuddin, Negative capacitance in a ferroelectric capacitor, Nat. Mater. **14**, 182 (2015).

[21] M. Hoffmann, M. Pešić, K. Chatterjee, A. I. Khan, S. Salahuddin, S. Slesazeck, U. Schroeder, and T. Mikolajick, Direct observation of negative capacitance in polycrystalline ferroelectric HfO_2, Adv. Funct. Mater. **26**, 8643 (2016).

[22] M. Hoffmann, M. Pešić, S. Slesazeck, U. Schroeder, and T. Mikolajick, On the stabilization of ferroelectric negative capacitance in nanoscale devices, Nanoscale **10**, 10891 (2018).

[23] D. J. R. Appleby, N. K. Ponon, K. S. K. Kwa, B. Zou, P. K. Petrov, T. Wang, N. M. Alford, and A. OŃeill, Experimental observation of negative capacitance in ferroelectrics at room temperature, Nano Lett. **14**, 3864 (2014).

[24] W. Gao, A. Khan, X. Marti, C. Nelson, C. Serrao, J. Ravichandran, R. Ramesh, and S. Salahuddin, Room-temperature negative capacitance in a ferroelectric-dielectric superlattice heterostructure, Nano Lett. **14**, 5814 (2014).

[25] A. K. Saha, S. Datta, and S. K. Gupta, "Negative capacitance" in resistor-ferroelectric and ferroelectric-dielectric networks: Apparent or intrinsic? J. Appl. Phys. **123**, 105102 (2018).

[26] S. J. Song, Y. J. Kim, M. H. Park, Y. H. Lee, H. J. Kim, T. Moon, K. D. Kim, J.-H. Choi, Z. Chen, A. Jiang *et al.*, Alternative interpretations for decreasing voltage with increasing charge in ferroelectric capacitors, Sci. Rep. **6**, 1 (2016).

[27] F.-C. Sun, M. T. Kesim, Y. Espinal, and S. P. Alpay, Are ferroelectric multilayers capacitors in series? J. Mater. Sci. **51**, 499 (2016).

[28] L. Pintilie, C. Ghica, C. M. Teodorescu, I. Pintilie, C. Chirila, I. Pasuk, L. Trupina, L. Hrib, A. G. Boni, N. G. Apostol *et al.*, Polarization induced self-doping in epitaxial $Pb(Zr_{0.20}Ti_{0.80})O_3$ thin films, Sci. Rep. **5**, 14974 (2015).

[29] I. Pintilie, C. M. Teodorescu, C. Ghica, C. Chirila, A. G. Boni, L. Hrib, I. Pasuk, R. Negrea, N. Apostol, and L. Pintilie, Polarization-control of the potential barrier at the electrode interfaces in epitaxial ferroelectric thin films, ACS Appl. Mater. Interfaces **6**, 2929 (2014).

[30] A. P. Levanyuk, B. A. Strukov, and A. Cano, Background dielectric permittivity: Material constant or fitting parameter? Ferroelectrics **503**, 94 (2016).

[31] G. A. Boni, C. F. Chirila, L. Hrib, R. Negrea, L. D. Filip, I. Pintilie, and L. Pintilie, Low value for the static background dielectric constant in epitaxial PZT thin films, Sci. Rep. **9**, 1 (2019).

[32] J. Li, B. Nagaraj, H. Liang, W. Cao, C. C. Lee, and R. Ramesh, Ultrafast polarization switching in thin-film ferroelectrics, Appl. Phys. Lett. **84**, 1174 (2004).

[33] M. J. Highland, T. T. Fister, M.-I. Richard, D. D. Fong, P. H. Fuoss, C. Thompson, J. A. Eastman, S. K. Streiffer, and G. B. Stephenson, Polarization Switching without Domain Formation at the Intrinsic Coercive Field in Ultrathin Ferroelectric $PbTiO_3$, Phys. Rev. Lett. **105**, 167601 (2010).

[34] C.-L. Jia, V. Nagarajan, J.-Q. He, L. Houben, T. Zhao, R. Ramesh, K. Urban, and R. Waser, Unit-cell scale mapping of ferroelectricity and tetragonality in epitaxial ultrathin ferroelectric films, Nat. Mater. **6**, 64 (2007).